IEEE Photonics Journal
An IEEE Photonics Society Publication

Open Access

An Efficient Method for Offset Mitigation in Free-Space Optical Systems

Volume 11, Number 4, August 2019

Omar A. Saraereh
Imran Khan
Jeong Woo Lee

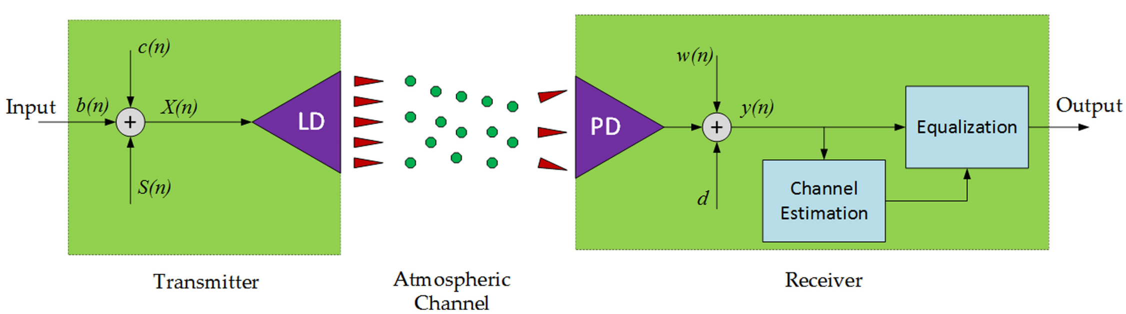

DOI: 10.1109/JPHOT.2019.2926126

An Efficient Method for Offset Mitigation in Free-Space Optical Systems

Omar A. Saraereh,[1] **Imran Khan**,[2] **and Jeong Woo Lee**[3]

[1]Communications Engineering Department, King Abdullah II School of Engineering, Princess Sumaya University for Technology, Amman 11941, Jordan
[2]Department of Electrical Engineering, University of Engineering & Technology, Peshawar 814, Pakistan
[3]School of Electrical and Electronics Engineering, Chung-Ang University, Seoul 156-756, South Korea

DOI:10.1109/JPHOT.2019.2926126
This work is licensed under a Creative Commons Attribution 4.0 License. For more information, see https://creativecommons.org/licenses/by/4.0/

Manuscript received June 7, 2019; revised June 22, 2019; accepted June 27, 2019. Date of publication July 1, 2019; date of current version July 18, 2019. This work was supported in part by the Chung-Ang University research grant in 2017 and in part by the Basic Science Research Program through the National Research Foundation of Korea funded by the Ministry of Education under Grant NRF-2016R1D1A1B03933174. Corresponding author: Jeong Woo Lee (e-mail: jwlee2@cau.ac.kr).

Abstract: Channel estimation is a key feature for free space optical (FSO) wireless communication systems which are required for a high QoS and high data rate system. Aiming at the problem of FSO wireless channel estimation, this paper proposes an implicit sequence channel estimation scheme to eliminate dc offset, and studies the key factors affecting the system performance. The optimal power allocation factor is derived based on the maximum SNR criterion. The system performance parameters such as the bit error rate (BER), mean square error (MSE), and computational complexity are evaluated. The results show that under the same dc bias condition, the MSE is estimated to decrease significantly after using the method of this paper. With the increase of dc offset d, the system error rate is significantly reduced and more approaching $d = 0$ (i.e., no dc offset). The proposed algorithm effectively mitigates the dc offset impact on the system and the BER is significantly improved while the MSE is reduced to 50% of the traditional state-of-the-art method. The proposed work can provide a technical solution to the FSO system and give support to technological development.

Index Terms: FSO, system performance, BER, turbulence, channel estimation.

1. Introduction

The wireless optical communication system uses light as an information carrier for data transmission, and has the characteristics of frequency bandwidth, large communication capacity, strong anti-interference, and the like, and does not interfere with electronic equipment, and can be applied to homes and offices. Therefore, indoor wireless optical communication technology has gradually received attention [1]. Implicit Training (IT) channel estimation is a channel estimation method that superimposes training sequence algebra on information sequences [2]–[5]. Commonly used blind channel estimation [6], [7] and channel estimation training sequence (TS) based [5]–[12] compared to its no extra bandwidth, and the receiving terminal only with an order statistical property can be training sequence is isolated. The method can effectively improve the utilization of bandwidth, and at the same time avoids the problems of high complexity and difficulty in implementation when using high-order statistical characteristics. Therefore, introducing the implicit sequence channel estimation method into wireless optical communication and using it to estimate the channel state information has certain advantages.

The performance of implicit sequence channel estimation is constrained by factors such as power allocation and data information. Literature [2], [3] studies the problem of data information input noise interference in optical IT channel estimation. Literature [4], [5] studies the effect of power allocation on optical IT channel estimation, and clearly indicates that non-optimal power allocation factors can lead to system performance degradation. In the actual environment, due to the unsatisfactory receiver, the application of the first-order statistical characteristics for channel estimation introduces the unknown DC offset (DCO), which affects the estimation result more than the power allocation, data information, and other parameters. The impact on estimated performance is even more serious. To this end, researchers have conducted research on how to eliminate the DCO problem [13], [15]. Among them, in [13], based on the unbiased estimation of optical IT channel, a DCO estimation algorithm is proposed by constructing the cost function of DCO. In [14], for the optical orthogonal frequency division multiplexing (OFDM) system, a method for directly estimating the received signal by using the statistical correlation of the transmitted signal is proposed, thereby avoiding the interference of the DCO in the zero carriers. In [15], for the asymmetric shaping DFDMA (CO-OFDM) system, an algorithm for simultaneously eliminating DCO and system noise is proposed by using the concept of Virtual Clean Window (VCW). The authors in [16] proposed a dual-hop blind detection FSO system over a log-normal channel. The improved CSI is obtained using a relay using such algorithm. However, the proposed algorithm lacks to consider the adaptive window length and synchronization. It only compares its results with a direct link. The author in [17] compares DCO-OFDM, ACO-OFDM and U-OFDM schemes in underwater optical communication systems. They study the distortions caused by the peak power and optimize the modulation index and compromise the clipping effects and SNR. By optimizing the SNR, the achievable transmission distance is obtained by the given transmission bit rate and BER performance. However, the proposed comparative review does not consider the other important aspect of FSO such as the frequency offset, DCO based on implicit training sequence and energy efficiency. The authors in [18] proposed a photon-counting underwater OWC system. They proposed a joint source-channel coding scheme for high BER video transmission. They consider the AMR and BER for analysis of video frames provided that the measurement rate is large enough. This study only focuses on the above aspect of FSO and does not consider the channel estimation impairments aspects. The authors in [19] propose two pilot-based linear channel estimation schemes for FSO systems. They are LS and MMSE in the frequency domain. The study compares the Mean Square Error (MSE) and complexity of both algorithms and evaluated the relative benefits of each algorithm. However, the study does not consider the offset impairments problems in the FSO systems. In [20], the authors propose a new modified compressed sensing (CS) based channel estimation algorithm SS-SAMP for the ACO-OFDM FSO system. The performance was evaluated in terms of BER, MSE, computational complexity, nonlinearity, and channel response. The results show that the proposed algorithm performs better than the traditional LS-based method. The proposed study only focused on the ACO-OFDM FSO whereas it does not consider another key aspect of FSO systems, such as the DCO-OFDM channel impairments and turbulence analysis. The authors in [21] investigated the performance of SM-UOMIMO system with FDAPPM scheme and adaptive PAA. The apply OC EGC or SC for MLSD. The results indicate that the OC provides a notable performance improvement compare with EGC and SC but it requires the highest computational complexity in practice. Moreover, the proposed study performance degrades with the destructive effect of ISI even in high SNR conditions. The authors in [22] present an experimental demonstration of a 2×2 MIMO-OFDM UWOC system. Two commercially available LEDs and two 10 MHz photodiodes were used as transmitters and receivers, respectively. The gross bit rate of the system is analyzed after 2 m fresh tap water channel transmission. The measured BERs within a wide reception area is below the FEC threshold. As a result, the system can achieve reliable data transmission for a relatively large reception area. The proposed study focused on the MIMO FSO system in underwater wireless channel analysis. It does not consider the DCO problems in the FSO systems and other important channel parameters. The authors in [23] a unified hybrid channel coding scheme

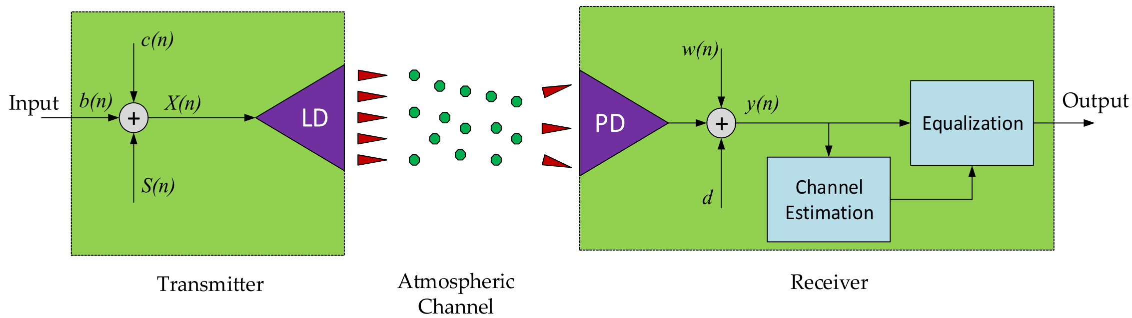

Fig. 1. Proposed implicit training FSO system model for channel estimation.

constituted by concatenation of irregular LDPC and TCM codes of ½ rate. The results are compared with the conventionally used channel coding schemes under weak turbulence conditions. However, this study does not take into account the strong turbulence, synchronization, LoS, noisy conditions and offset analysis.

Although the above method better eliminates the influence of DCO on channel estimation, there are defects such as high complexity or slow convergence speed in different degrees. In this paper, an implicit sequence channel estimation method for eliminating DCO is proposed to improve the estimation performance of channel state parameters of optical communication systems.

2. Proposed FSO System Model for Channel Estimation

The proposed implicit series FSO channel estimation scheme is shown in Figure 1.

In Figure 1, $b(n)$ denotes a sequence of information whose average power is $E[|b(n)|^2] = \sigma_b^2$; $c(n)$ denotes a training sequence of period T (i.e satisfying $c(n) = c(n+T)$), the average power is $\sigma_c^2 = (\frac{1}{T})\sum_{i=0}^{T-1}|c(i)|^2$. The total power of the system is $\sigma_b^2 + \sigma_c^2 = q$. Assuming that the transmitted signal $X(n)$ is superposed by $b(n)$ and $c(n)$ algebra, that is, $X(n) = b(n) + c(n)$, then the received signal $y(n)$ can be expressed as:

$$y(n) = \sum_{l=0}^{L-1} h(l)\, x(n) + w(n) + d \tag{1}$$

In Equation (1), L represents the channel order, $h(l)$ represents the l channel coefficient order, d represents the DC bias, $w(n)$ represents the noise of the detector and can be equivalent to Gaussian white noise. Let it satisfy $w(n) \sim N(m, \sigma_n^2)$, $m \geq 0$, and $E\{[w(n+\tau) - m][w(n) - m]^H\} = \sigma_n^2 \boldsymbol{I}_N \delta(\tau)$, where N represents the length of the received data symbol. Substituting $x(n)$ in Equation (1) we get:

$$y(n) = \sum_{l=0}^{L-1} h(l)\,[b(n-l) + c(n-l)] + w(n) + d \tag{2}$$

In order to perform channel estimation using the first-order statistical characteristics of the received signal, first, the received signal $y(n)$ in Equation (2) is sampled and averaged by the period T, and:

$$r(n) = E[y(kT+n)], \quad n = 0, 1, \ldots, \left(\frac{N}{T} - 1\right) \tag{3}$$

Equation (3) can be rewritten as:

$$r(n) = E\left[\sum_{l=0}^{L-1} h(l)\, b(kT+n-l)\right] + E\left[\sum_{l=0}^{L-1} h(l)\, c(kT+n-l)\right] + E[w(kT+n)] + E[d] \tag{4}$$

In Equation (4), assuming that the statistical mean of $b(n)$ and $w(n)$ is known, the mathematical expectation of items 1 and 3 is constant. Then we can simplify Equation (4) to:

$$\hat{r}\,(n) = d + \sum_{l=0}^{L-1} h\,(l)\,c(n-l)_T, \quad n = 0, 1, \ldots, T-1 \tag{5}$$

Among them, $(\cdot)_T$ defines the arithmetic modulo T operation. The unbiased estimation of the channel coefficients in Equation (5) has a unique solution condition of $T = L$ and requires the coefficient matrix of the training sequence to be full rank [24]. In fact, only the upper bound of the channel order must be known in the estimation process, and $T \geq L$ is selected, and the algorithm can still guarantee a unique solution. Only in the absence of DCO, the following T-L solutions $h(L)$, $h(L+1), \ldots, h(T-1)$ are all zero. The matrix form of Equation (5) is:

$$\hat{\boldsymbol{r}} = \boldsymbol{C}\boldsymbol{h} + \boldsymbol{d} \tag{6}$$

In Equation (6), $\hat{\boldsymbol{r}} = [\hat{r}(T-1),\ \hat{r}(T-2), \ldots,\ \hat{r}(0)]^T_{T\times 1}$; $\boldsymbol{h} = [h(T-1),\ h(T-2), \ldots,\ h(0)]^T_{T\times 1}$; $\boldsymbol{d} = [d,\ d, \ldots,\ d]^T_{T\times 1}$ and $\boldsymbol{C}$ is expressed as:

$$\boldsymbol{C} = \begin{bmatrix} c\,(0) & c\,(1) & c\,(2) & \cdots & c\,(T-1) \\ c\,(T-1) & c\,(0) & c\,(1) & \cdots & c\,(T-2) \\ c\,(T-2) & c\,(T-1) & c\,(0) & \cdots & c\,(T-3) \\ \vdots & \vdots & \vdots & \ddots & \vdots \\ c\,(1) & c\,(2) & c\,(3) & \cdots & c\,(0) \end{bmatrix}_{T\times T} \tag{7}$$

It can be known from Equation (6) that the channel estimation value affected by the DCO at this time can be recorded as:

$$\hat{\boldsymbol{h}}_d = C^{-1}\hat{\boldsymbol{r}} = \boldsymbol{h} + C^{-1}d \tag{8}$$

It can be known from Equation (8) that when the DCO does not exist (i.e., $d = 0$), the estimated value of the channel is the true value of the channel state, and when the DCO is present, the estimation result of the channel is inaccurate due to the influence of DC. If the value of the DCO can be accurately estimated, the influence of the DCO can be eliminated and accurate Channel State Information (CSI) can be obtained. To this end, based on the estimation of the mean value of the received signal samples, the DCO offset is estimated by using the correlation between the CSI and the DC offset. Assuming the length of the received data symbol is $N = TN_q$, the sample estimate of the average received signal for N_q samples is:

$$\hat{r}\,(N) = \frac{1}{N_q}\sum_{k=0}^{q} y\,(kT+n) \tag{9}$$

It is assumed that the received data $y(n)$ has no synchronization deviation. It can be seen from the previous analysis that when $T > L$, the channel coefficients $h(L), h(L+1), \ldots, h(T-1)$ are all zero and without DC bias. The channel coefficients when the DC offset is present are non-zero. At this point, the non-zero value can be considered to be caused by the DC offset, so the DC offset can be approximated as:

$$\hat{d} \approx \frac{h\,(L) + h\,(L+1) + \cdots + h\,(T-1)}{T-L} \tag{10}$$

Substituting the estimated values of Equations (9) and (10) into Equation (6) and rewriting it to:

$$\hat{\boldsymbol{r}} = \boldsymbol{C}\left[\boldsymbol{h}_{[L]} \quad 0_{(T-L)\times 1} + \hat{d} \times 1_{T\times 1}\right] \tag{11}$$

Among them, $\boldsymbol{h}_{[L]} \quad 0_{(T-L)\times 1}$ represents the channel impulse response (CIR) vector, and $[h_L,\ h_{L+1}, \ldots,\ h_{T-1}]^T$ and zero vector, $\hat{d} = \frac{d}{sum(c)}$, $sum(c) = c(0) + c(1) + \cdots + c(T-1)$. Simplifying

Equation (11) we get:

$$\boldsymbol{C}^{-1}\hat{\boldsymbol{r}} = \left[\boldsymbol{h}_{[L]} \quad 0_{(T-L)\times 1}\right] + \hat{d} \times 1_{T\times 1} \tag{12}$$

At this point, the channel state parameters for eliminating the DC offset are:

$$\hat{\boldsymbol{h}} = \left[\boldsymbol{C}^{-1}\hat{\boldsymbol{r}}\right] - \hat{d} \tag{13}$$

It can be known from Equation (13) that the accuracy of the channel state parameter estimation is directly affected by the DCO. The higher the accuracy of the DCO estimation, the more accurate the estimate of the channel state parameters.

3. Performance of Implicit Sequence Channel Estimation

3.1 MSE Calculation

Assume that the DC offset has been accurately estimated, i.e., $d \approx \hat{d}$. Then, without considering the DC offset, Equation (2) can be converted into:

$$y(n) = \sum_{l=0}^{L-1} h(l)\left[b(n-l) + c(n-l)\right] + w(n) \tag{14}$$

Combined with (13):

$$\hat{h} = \frac{1}{N_q}\sum_{k=0}^{N_q-1}\left[\boldsymbol{C}^{-1}\boldsymbol{h}b(kT) + \boldsymbol{C}^{-1}\boldsymbol{h}c(-kT) + \boldsymbol{C}^{-1}w(kT)\right] - \hat{d} \tag{15}$$

At this point, the channel estimation deviation is:

$$e = \hat{h} - h = \frac{1}{N_q}\sum_{k=0}^{N_q-1}\left[\boldsymbol{C}^{-1}\boldsymbol{h}b(kT) + \boldsymbol{C}^{-1}w(kT)\right] - \hat{d} \tag{16}$$

The corresponding channel MSE is:

$$\sigma_e^2 = E\left[\left|\hat{h} - h\right|^2\right] = E\left[|e|^2\right] = tr\left\{E\left[ee^H\right]\right\} \tag{17}$$

Among them,

$$E\left[ee^H\right] = \frac{1}{N_q^2}\sum_{i=0}^{N_q-1}\sum_{j=0}^{N_q-1}\boldsymbol{C}^{-1}\boldsymbol{h}\left[b(iT)b^H(jT)\right]\boldsymbol{h}^H\boldsymbol{C}^{-H} + \frac{1}{N_q^2}\sum_{i=0}^{N_q-1}\sum_{j=0}^{N_q-1}\boldsymbol{C}^{-1}\left[w(iT)w^H(jT)\right]\boldsymbol{C}^{-H} + \left|\hat{d}\right|^2 \tag{18}$$

Then Equation (17) can be converted into:

$$\begin{aligned}\sigma_e^2 &= \frac{1}{N_q}\frac{\sigma_b^2}{\sigma_c^2}\cdot tr\left\{\boldsymbol{C}^{-1}\boldsymbol{h}\boldsymbol{h}^H\boldsymbol{C}^{-H}\right\} + \frac{N_q-1}{N_q^2}\cdot\frac{\sigma_b^2}{\sigma_c^2}\cdot tr\left\{\boldsymbol{C}^{-1}\boldsymbol{h}J^+h^H C^{-H}\right\} + \frac{1}{N_q}\frac{\sigma_b^2}{\sigma_c^2}\cdot tr\left\{C^{-1}C^{-H}\right\} + \left|\hat{d}\right|^2 \\ &= \frac{1}{N_q}\frac{\sigma_b^2 + \sigma_n^2}{\sigma_c^2} + \left|\hat{d}\right|^2\end{aligned} \tag{19}$$

In Equation (18), $J^+ = J_{(2P-1)} + J_{(2P-1)}^T$, and $J = semicric(0, 0, \ldots, 1, 0, \ldots, 0)$, $semicric(\cdot)$ indicates that a semi-circular matrix operation is generated, with only 1 element appearing at the $(T+1)$ position and all other positions being 0. Define $P = \frac{\sigma_c^2}{(\sigma_b^2+\sigma_c^2)}$ as the power allocation factor, $\gamma = \frac{(\sigma_b^2+\sigma_c^2)}{\sigma_n^2}$ is the pre-equalization SNR, then Equation (19) can be transformed for:

$$\sigma_e^2 = \frac{1}{N_q}\cdot\left(\frac{1}{P} - 1 + \frac{1}{P\gamma}\right) + \left|\hat{d}\right|^2 \tag{20}$$

It can be seen from Equation (20) that the MSE of the channel estimate is subject to N_q (i.e., the data symbol length N is related to the training sequence period T), the power allocation factor P, the pre-equalization SNR γ, and the DC offset estimate $\hat{d}$ impact. When N and T are fixed, the MSE of the channel estimation is mainly related to the power allocation factor P, the pre-equalization SNR γ, and the DC offset estimation value $\hat{d}$. When γ is large, then $\frac{1}{P\gamma} \to 0$, so Equation (20) can be converted into:

$$\sigma_e^2 \approx \frac{1}{N_q} \cdot \left(\frac{1}{P} - 1 \right) + \left| \hat{d} \right|^2 \tag{21}$$

It can be known from Equation (21) that the MSE at this time is only related to the data symbol length N, the training sequence period T, the power allocation factor P, and the DC offset estimation value $\hat{d}$, regardless of γ, that is, MSE performance is not affected by γ. When N, T and $\hat{d}$ is present, the power allocation factor P is a key factor affecting the performance.

3.2 Power Allocation Problem in Implicit Sequence Channel Estimation

In the IT channel estimation, when the total power q of the system is constant, the power allocation between the training sequence and the corresponding information sequence will directly affect the accuracy of the channel parameter estimation and system performance. When the power obtained by the training sequence is large, although the channel estimation accuracy is improved, the power obtained by the information sequence is small, which may cause the system error rate to increase [25]. On the contrary, the power obtained by the training sequence is smaller. This affects the accuracy of the estimate, which also causes an increase in the system error. Therefore, choosing the right power allocation factor is the key. In order to optimize the error performance of the system after equalization, this paper uses the output SNR maximum criterion to obtain the optimal power allocation factor [26]. The assumptions in the analysis process are as follows:

1) It is assumed that the channel coefficient $h(l)$ is a random variable satisfying the variance $(\frac{1}{T})$, and satisfies $h_i(l) \neq h_m(k)$ when $i \neq m$, $k \neq l$ irrelevant to each other.
2) Combining Equations (3) and (8), it is known that when $N_q \to \infty$ (i.e., $N \to \infty$), $\hat{r}(n) \to r(n)$.

According to Equation (1), the received signal of the removal training sequence and the DC offset portion is:

$$\hat{y}(n) = y(n) - \sum_{l=0}^{L-1} \hat{h}(l)\, c(n-l) - \hat{d} \tag{22}$$

If the DC offset has been accurately estimated, i.e., $d \approx \hat{d}$ and substituting Equation (2) into Equation (22):

$$\hat{y}(n) \approx \sum_{l=0}^{L-1} \hat{h}(l)\, b(n-l) + \sum_{l=0}^{L-1} \left[h(l) - \hat{h}(l) \right] \left[b(n-l) + c(n-l) \right] + w(n) \tag{23}$$

In Equation (23), $X_s = \sum_{l=0}^{L-1} \hat{h}(l) b(n-l)$ indicates a valid signal, $v(n) = \sum_{l=0}^{L-1} [h(l) - \hat{h}(l)] [b(n-l) + c(n-l)] + w(n)$ represents the sum of the noise interference after equalization, which consists of the channel estimation deviation term and the input noise term at the receiving end before equalization. Then, after channel equalization, the output SINR can be expressed as:

$$SINR = \frac{\sigma_{X_s}^2}{\sigma_v^2} \tag{24}$$

Where $\sigma_{X_s}^2$ represents the average power of the effective signal X_s and σ_v^2 represents the average power of the equalized noise signal $v(n)$. The detailed derivation is as follows:

1) Power of the effective signal

Known by the assumption (2), $\lim_{N\to\infty} E\{\hat{r}(n)\} = r(n)$, satisfying $\lim_{N\to\infty} E\{\hat{\boldsymbol{h}}|\boldsymbol{h}\} = \boldsymbol{h}$ established. Then the average power of the effective signal X_s can be expressed as:

$$\begin{aligned}\sigma_{X_s}^2 &= E\left[X_s(n)^2\right] \\ &= E\left[\left\|\sum_{l=0}^{L-1} \hat{h}(l)\, b(n-l)\right\|^2\right] \\ &= \sigma_b^2 .tr\left\{E_h\left\{E\left\{\hat{\boldsymbol{h}}\hat{\boldsymbol{h}}^H|\boldsymbol{h}\right\}\right\}\right\} \\ &= \sigma_b^2 .tr\left\{E_h\left\{cov\left(\hat{\boldsymbol{h}}, \hat{\boldsymbol{h}}|\boldsymbol{h}\right) + \boldsymbol{h}\boldsymbol{h}^H\right\}\right\} \\ &= \sigma_b^2\left(\sigma_e^2 + 1\right)\end{aligned} \tag{25}$$

The hypothesis (1) is used in the derivation of Equation (25), $tr\{\cdot\}$ represents the trace operation of the matrix, and $(\cdot)^H$ represents the conjugate transpose of the matrix.

2) The sum of the noise signal after equalization

The average power of the equalized noise signal $v(n)$ can be expressed as:

$$\begin{aligned}\sigma_v^2 &= \frac{1}{N}\sum_{n=0}^{N-1} = E\left[v(n)^2\right] \\ &= \sigma_b^2.\sigma_e^2 + N\sigma_n^2 + \frac{\sigma_n^2}{N}\sum_{n=0}^{N-1}\sum_{l_1=0}^{L-1}\sum_{l_2=0}^{L-1} E\left\{\left[h(l_1) - \hat{h}(l_1)\right]\left[h(l_2) - \hat{h}(l_2)\right]\right\}.\bar{c}^*(n-l_1)\,\bar{c}(n-l_2)\end{aligned} \tag{26}$$

In Equation (26), defined $\bar{c}(n) = \sigma_c^{-1} c(n)$. Assuming that this paper uses an m-sequence with good autocorrelation properties, Equation (26) can be simplified as:

$$\sigma_v^2 \approx \sigma_e^2\left(\sigma_b^2 + \sigma_c^2\right) + N\sigma_n^2 \tag{27}$$

It can be seen from Equation (27) that the power of the summed noise is related to the average power σ_n^2 input noise before equalization and the channel estimation MSE σ_e^2. Wherein, the MSE σ_e^2 has been obtained in the foregoing deviation, and the power of the input pre-equalization noise can be obtained by a method based on threshold decision and sequence separation [17], [23], [26].

3) Acquisition of optimal power allocation factor

Substituting the results of Equations (25) and (27) into Equations (24), the expression about the power allocation factor can be obtained after finishing:

$$SINR(P) = \frac{\sigma_{X_s}^2}{\sigma_v^2} = \frac{f_1 P^2 + f_2 P + f_3}{g_1 P + g_2} \tag{28}$$

Wherein the parameters f_1, f_2, f_3, g_1, g_2 are defined as:

$$\begin{cases} f_1 = q(T-N) \\ f_2 = q(N-2T) - T\sigma_n^2 \\ f_3 = T\left(q + \sigma_n^2\right) \\ g_1 = N^2\sigma_n^2 - qT \\ g_2 = T\left(q + \sigma_n^2\right)\end{cases} \tag{29}$$

For the first-order derivation of P for Equation (28) and taking the positive root of the Equations, the optimal power allocation factor can be obtained.

$$P_0 = \frac{g_2}{g_1}\left[-1+\sqrt{1+\frac{g_1\left(f_3 g_1 - f_2 g_2\right)}{g_2^2 f_1}}\,\right] \tag{30}$$

At the same time, the input SNR $\gamma = \frac{(\sigma_b^2+\sigma_c^2)}{\sigma_n^2}$ substituted into Equation (30), then the optimal power allocation factor can be expressed as:

$$P_0 = \frac{T(\gamma+1)}{N^2-\gamma.T}\left\{1+\sqrt{-1+\frac{\left(N^2-\gamma.T\right)\left[N^2+T+\gamma(T-N)\right]}{T.\gamma(N-T)(\gamma+1)}}\,\right\} \tag{31}$$

At this time, the maximum output SINR after equalization is:

$$SINR_0 = \frac{\gamma(T-N)P_0^2+\left[\gamma(N-2T)-T\right]P_0+T(\gamma+1)}{\left(N^2-\gamma.T\right)P_0+T(\gamma+1)} \tag{32}$$

And from Equations (31) and (32), the optimal power allocation factor and the maximum output SNR equalized data symbols not only the length of N, training sequence period T, but also with the front end of the receiver input SNR equalization γ has a close relationship. For example, when $N = 600$, $T = 15$ is fixed, γ takes 12 dB to obtain the theoretical value $P_0 \approx 0.2$ of the optimal power allocation factor, and the maximum output SNR after equalization is $SINR_0 \approx 4.58$ dB. When γ takes 14 dB so the optimal power allocation factor also satisfies $P_0 \approx 0.2$, where $SINR_0 \approx 7.08$ dB.

4. Experimental Results

In order to better illustrate the effectiveness and feasibility of the proposed method, the channel order L case is known to 4PPM modulation, for example, are given the MSE method, the bit error rate, and the algorithm complexity performance. Wherein, the channel order $L = 6$, the data block length $N = 600$, and the training sequence uses the m sequence of the period $T = 15$, that is, $c(n) = \{1, 0, 0, 0, 1, 1, 1, 1, 0, 1, 0, 1, 1, 0, 0\}$. The channel coefficient matrix is taken as $\boldsymbol{h}_1 = [0.7221, 0.3560, 0.1749, 0.0859, 0.0487, 0.0346]$. The parameter is at a laser wavelength of 3.8 μm, visibility and transmission distance are 1 km and 1.5 km, respectively. The impulse response is sampled at a symbol period of 5 ns [27]. First, the normalized MSE is used to measure the channel estimation performance, which is expressed as:

$$\boldsymbol{E}_{MSE} = \left(\frac{1}{M}\right)\sum_{i=1}^{M}\frac{\left(\hat{\boldsymbol{h}}_i-\boldsymbol{h}^2\right)}{\boldsymbol{h}^2} \tag{33}$$

Where M is the number of Monte Carlo simulations for each experiment.

Figure 2 depicts the effect of the power allocation factor on the MSE of the channel estimation. It can be seen from Figure 2 that when the SNR γ is equal before the equalization, the MSE of the estimated value will decrease as the power allocation factor increases. It is worth noting that when $\gamma > 16$ dB, the MSE curve almost coincides, and γ is no longer an important factor affecting the MSE performance, which is consistent with the theoretical analysis of Equation (21). Such results give a clear idea that if we configure to a certain threshold value of γ, then we can definitely get freedom from it and the system MSE performance will not be affected by it and the channel estimation performance will be of an acceptable level.

In order to verify the rationality of theoretical analysis, to study an example 4PPM modulation factor before and after the equalization output SNR and power allocation factor P relationship, which results in Figure 3. Figure 3 is a post-equalized output signal to interference and noise ratio (*SINR*) with P curve, then $N = 600$ and $T = 15$. It can be seen from Figure 3 that when the power allocation factor takes values in (0.1, 0.5), the SINR is relatively large, because the information sequence in the transmitted signal obtains more power and enhances the strength of the data

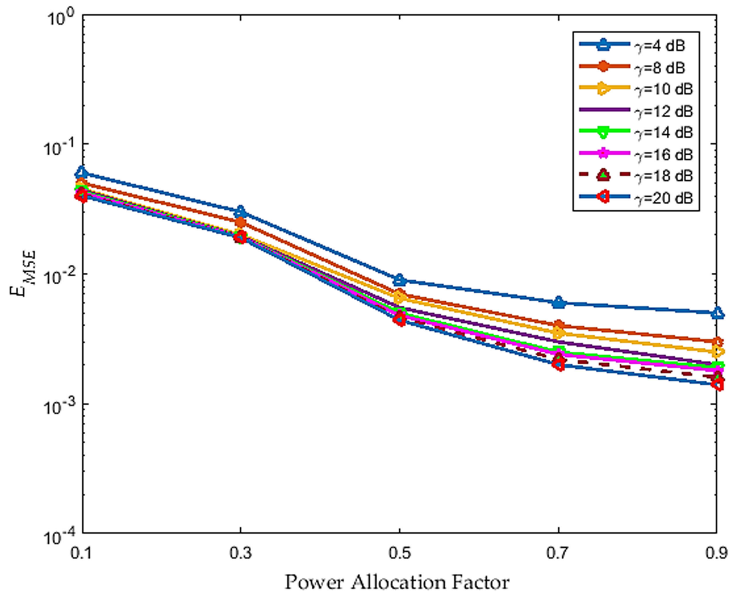

Fig. 2. Analysis of MSE versus different power allocation factors under various SNRs γ.

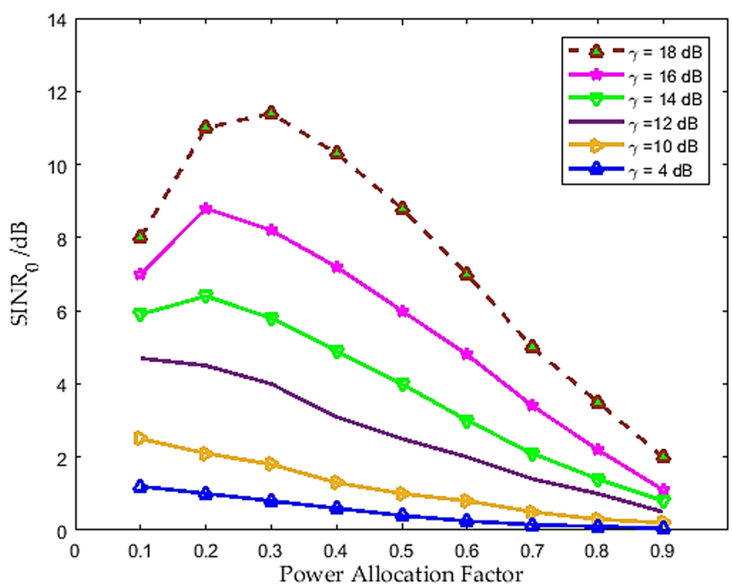

Fig. 3. SINR versus power allocation factor after equalization.

signal in the receiving end. Meanwhile, the maximum output SINR after equalization algorithm is focused on this $P = 0.2$ nearby, and the $\gamma = 12$ dB and 14 dB, respectively the $SINR_0 \approx 4.7$ dB and *the* $SINR_0 \approx 6.7$ dB, and the analysis is basically the same. In particular, the following simulation experiments were carried out based on the optimal power allocation factor $P_0 = 0.2$. Such results give an idea about how to acquire certain SINR for the system under consideration by variation of the γ and power allocation factor.

Figure 4 shows the relationship between the E_{MSE} of the proposed algorithm and the pre-equalization SNR. The curves d ($d \neq 0$) and D_1 in Figure 4 represent the E_{MSE} curve after the DC offset is not eliminated and the DC offset [24] is removed. It can be seen from Figure 4 that:

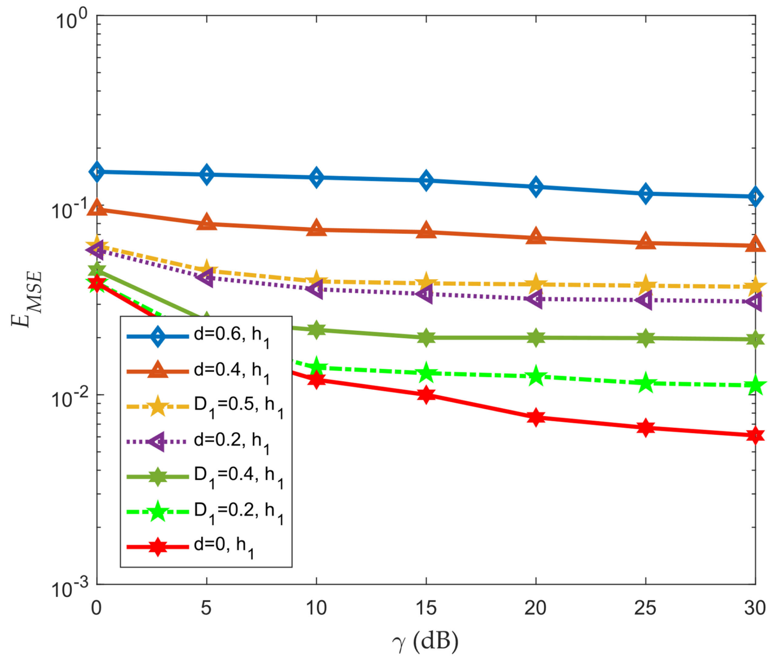

Fig. 4. MSE analysis under $\boldsymbol{h}_1$ channel parameter with different dc offsets.

1) Using the proposed DCO method, the MSE of the system is significantly reduced, and with the increase of the DC offset d, the improvement of the MSE performance after eliminating the DC offset is more obvious, that is, more close to no DC bias. For example, the curve at $D_1 = 0.2$ and the curve at $d = 0$ almost coincide.
2) As the SNR increases, the MSE decreases significantly. Moreover, when the SNR is large, the estimated E_{MSE} will tend to a certain value, which is consistent with the theoretical analysis in equation (21) and the simulation results in Figure 2.
3) With the increase of DC offset, although the MSE of the system is also increasing, compared with the case of no DC offset, the MSE reduction after using the proposed method is the no DC offset [24] is twice as much. This shows that the proposed method can significantly reduce the impact of DC bias on system performance.

Such results collective gives us information on how to control the SNR to obtain the optimal MSE value of the FSO channel.

Figure 5 shows the BER of the system as a function of γ after the proposed method. The curves $d\,(d \neq 0)$ and D_1 in Figure 5 represents the BER curves for which the DC offset [24] is not eliminated and the DC offset is eliminated, respectively. It can be seen from Figure 5 that after using the proposed scheme, the BER of the system is significantly reduced, and with the increase of the DC offset d, the improvement of the error performance of the system after eliminating the DC offset is more obvious, that is, it is closer to $d. = 0$ (i.e., no DC offset). When the system BER is 4×10^{-3}, the γ is improved by 6 dB and 2 dB respectively before and after the equalization of the DC offset $d = 0.4$ and 0.2. This result again shows that the proposed method effectively eliminates the influence of DC offset on system performance and better estimate the FSO channel with improved CSI.

In addition to the MSE and the systematic BER, the computational complexity of the algorithm is the key to its promotion and application. Therefore, the complexity of the channel parameter estimation method proposed in this paper and the algorithm without the DC offset in the literature [24] are compared. The complexity comparison results of the two algorithms are listed in Table 1. Compared with the literature [24] algorithm, the complexity and running time of the proposed algorithm are decreased. Under the above simulation conditions, the number of addition and multiplication

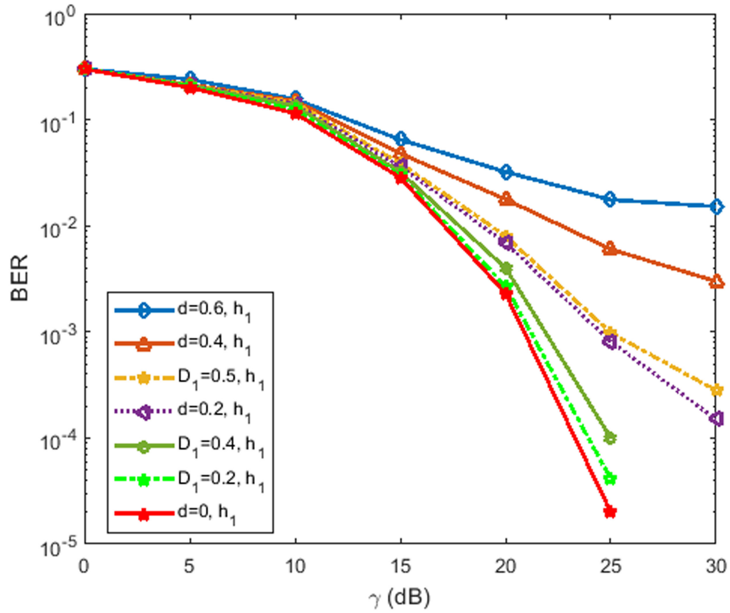

Fig. 5. BER analysis under h_1 channel parameter with different dc offsets.

TABLE 1
Computational Complexity Comparison of the Algorithms

Channel Estimation Algorithm		Proposed Algorithm with DCO	Reference [24] Algorithm without DC
Running Time (s)		35	37
Computational Complexity	Addition Times	$M[14N + N_q - 4T + 2T^2 + 4L + 32]$	$M[17N + 2N_q + T + 2T^2 + 3L + 33]$
	Multiplications Times	$M[4N + 2T + T^2 + NL + 21] + 26$	$M[4N + 3T + 2T^2 + NL + 21] + 26$

operations of the literature [16] algorithm are 1.080×10^7 times and 6.516×10^6 times and the number of addition and multiplication operations of the proposed method is 8.886×10^6 times and 6.276×10^6 times, respectively. The addition and multiplication complexity of the proposed scheme is decreased by 21.5% and 3.8%, respectively, and the overall computational complexity of the system decreased by 14.2%.

5. Conclusions

Aiming at the problem of wireless optical channel estimation, this paper proposes an implicit sequence channel estimation scheme to eliminate DC offset and studies the key factors affecting system performance. The results show that: (1) Under the same DC bias condition, the MSE is estimated to decrease significantly after using the method of this paper; (2) With the increase of DC offset d, the system error rate is significantly reduced and more Approaching $d = 0$ (i.e., no DC offset); (3) After the equalization, the output signal-to-noise ratio of the system varies with the power allocation factor, and the most favorable power allocation factor needs to be selected based on comprehensive consideration of system performance. Best system performance. It should be noted that from the perspective of the system performance of the simulation when the DC offset is large, the error rate of the system after DC offset is larger than the ideal state, and the DC offset and system noise are comprehensively considered. Eliminating the problem will be the next step that needs to be addressed. Under the optimal power allocation condition, when the bit error rate is 4×10^{-3}, the DC offset is 0.2 and 0.4 respectively, and the signal-to-noise ratio of the system is improved by about 2 dB and 6 dB, respectively. The computational complexity is decreased by 14.2%.

Acknowledgment

The authors declare no conflict of interest.

References

[1] I. Khan, “Channel modeling and analysis of OWC-massive MIMO Systems,” *Opt. Commun.*, vol. 434, pp. 209–217, 2018.
[2] H. P. Liu, H. Zhang, and C. J. Guo, “Channel estimation using data-dependent superimposed training for single-carrier coherent optical systems,” in *Proc. Asia Commun. Photon. Conf.*, 2013, paper AW3F.6.
[3] C. Zhu *et al.*, “Overhead-free channel estimation using implicit training for polarization-multiplexed coherent optical systems,” in *Proc. IEEE Opt. Fiber Commun. Conf. Expo. Nat. Fiber Opt. Eng. Conf.*, 2013, pp. 1–3.
[4] D. Wu *et al.*, “Channel estimation for asymmetrically clipped optical orthogonal frequency division multiplexing optical wireless communications,” *IET Commun.*, vol. 6, no. 5, pp. 532–540, 2012.
[5] H. Zhao *et al.*, “Compressed sensing theory-based channel estimation for optical orthogonal frequency division multiplexing communication system,” *Opt. Commun.*, vol. 326, pp. 94–99, 2014.
[6] S. J. Fan *et al.*, “Comparison of implicit training and implicit pilot in coherent optical transmission,” in *Proc. IEEE 12th Int. Conf. Opt. Internet*, 2014, pp. 1–2.
[7] A. Gorshtein *et al.*, “Blind channel estimation for MLSE receiver in high-speed optical communications: Theory and ASIC implementation,” *Opt. Exp.*, vol. 21, no. 19, pp. 21766–21789, 2013.
[8] M. Zamani *et al.*, “A blind channel estimation for 100+ Gb/s optical IM-DD DMT over 100-km SMF in 1550 nm,” *IEEE Photon. Technol. Lett.*, vol. vol. 26, no. 19, pp. 1928–1931, Oct. 2014.
[9] A. Nuuwanpriya *et al.*, “PAM-SCFDE for optical wireless communications,” *J. Lightw. Technol.*, vol. 33, no. 14, pp. 2938–2949, Jul. 2015.
[10] J. B. Wang *et al.*, “Complementary sequences-based channel estimation for diffuse wireless optical communications,” *Opt. Eng.*, vol. 50, no. 7, 2011, Art. no. 075003.
[11] X. Chen and M. Jiang, “Adaptive statistical bayesian MMSE channel estimation for visible light communication,” *IEEE Trans. Signal Process.*, vol. 65, no. 5, pp. 1287–1299, Mar. 2017.
[12] J. B. Wang *et al.*, “Training sequence based channel estimation for an indoor visible light communication system,” *Optoelectron. Lett.*, vol. 7, no. 3, pp. 213–216, 2011.
[13] J. B. Wang *et al.*, “Optimal training sequences for indoor wireless optical communications,” *J. Opt.*, vol. 14, no. 1, 2012, Art. no. 015401.
[14] X. Ma *et al.*, “Channel estimation for wideband underwater visible light communication: A compressive sensing perspective,” *Opt. Exp.*, vol. 26, no. 1, pp. 311–321, 2018.
[15] S. D. Dissanayake and J. Armstrong, “Novel techniques for combating DC offset in diversity combined ACO-OFDM,” *IEEE Commun. Lett.*, vol. 15, no. 11, pp. 1237–1239, Nov. 2011.
[16] M. Elbawab, M. Abaza, and M. H. Aly, “Blind detection for serial relays in free-space optical communication systems,” *Appl. Sci.*, vol. 8, no. 2074, pp. 1–10, 2018.
[17] J. Lian, Y. Gao, P. Wu, and D. Lian, “Orthogonal frequency division multiplexing techniques comparison for underwater optical wireless communication systems,” *Sensors*, vol. 19, no. 160, pp. 1–19, 2019.
[18] Z. Hong *et al.*, “Photon-counting underwater optical wireless communication for reliable video transmission using joint source-channel coding based on distributed compressive sensing,” *Sensors*, vol. 19, no. 1042, pp. 1–12, 2019.
[19] Y. S. Hussein, M. Y. Alias, and A. A. Abdulkafi, “On performance analysis of LS and MMSE for channel estimation in VLC systems,” in *Proc. IEEE 12th Int. Colloq. Signal Process. Appl.*, Melaka, Malaysia, 2016, pp. 204–209.
[20] M. T. Niaz, F. Imdad, W. Ejaz, and H. S. Kim, “Compressed sensing-based channel estimation for ACO-OFDM visible light communications in 5G systems,” *EURASIP J. Wireless Commun. Netw.*, vol. 268, pp. 1–14, 2016.
[21] A. Huang, L. Tao, and Y. Niu, “Underwater wireless optical MIMO system with spatial modulation and adaptive power allocation,” *Opt. Commun.*, vol. 412, pp. 21–27, 2018.
[22] Y. Song *et al.*, “Experimental demonstration of MIMO-OFDM underwater optical communication,” *Opt. Commun.*, vol. 403, pp. 205–210, 2017.
[23] R. Gupta, T. S. Kamal, and P. Singh, “Performance of OFDM: FSO communication system with hybrid channel codes during weak turbulence,” *J. Comput. Netw. Commun.*, vol. 2019, 2019, Art. no. 1306491.
[24] C. Gong and Z. Xu, “Channel estimation and signal detection for optical wireless scattering communication with inter-symbol interference,” *IEEE Trans. Wireless Commun.*, vol. 14, no. 10, pp. 5326–5337, Oct. 2015.
[25] X. T. Ling *et al.*, “Offset and power optimization for DCO-OFDM in visible light communication systems,” *IEEE Trans. Signal Process.*, vol. 64, no. 2, pp. 349–363, Jan. 2016.
[26] X. Zhou, C. Wang, and R. Tang, “Channel estimation based on IOTA filter in OFDM/OQPSK and OFDM/OQAM systems,” *Appl. Sci.*, vol. 9, no. 7, 2019, Art. no. 1454.